2002

The Behavior Of Gas Bubbles Entrained In The Liquid Film Of Horizontal Annular Flow

D. J. Rodriguez
University of Wisconsin-Madison

T. A. Shedd
University of Wisconsin-Madison

THE BEHAVIOR OF GAS BUBBLES ENTRAINED IN THE LIQUID FILM OF HORIZONTAL ANNULAR FLOW

*Daniel J. Rodríguez, Graduate Research Assistant, University of Wisconsin-Madison,
1500 Engineering Drive, Madison, WI 53706, USA; Tel.: 608/263-3346; Fax: 608/262-8464
E-Mail: rodrig@sel.me.wisc.edu *Author for Correspondence

Timothy A. Shedd, Assistant Professor, University of Wisconsin-Madison,
1500 Engineering Drive, Madison, WI 53706, USA; Tel.: 608/265-2930; Fax: 608/262-8464
E-Mail: shedd@engr.wisc.edu

ABSTRACT

Small entrained vapor bubbles can have a significant impact on the evaporation or condensation of a thin liquid film as may be found in the annular flow of refrigerant in a heat exchanger. For example, past work has indicated that unattached small vapor bubbles serve as sites for vaporization within a film that, on average, would be too thin to support nucleate boiling. Vapor entrained in a thicker film during condensation will effectively lower the resistance the film poses to heat transfer. In this work, the behavior of small air bubbles (on the order of 100 microns or less) in annular water films is studied using a variety of visualization techniques. The ultimate purpose is to understand the process of vapor entrainment and transport in the film. The mean size and concentration of bubbles are presented for a variety of stratified and annular flow conditions. In addition, particle tracking velocimetry (PTV) is used to find the velocities of gas bubbles moving within the film. PTV results show very complex behaviors, such as rapid accelerations and decelerations and corkscrew trajectories.

NOMENCLATURE

d: tube diameter [m]
g: gravitational acceleration [m/s^2]
F_t: Froude rate
W_g: air mass flow rate [kg/s]
W_l: water mass flow rate [kg/s]
U_{sg}: superficial gas velocity [m/s]
τ_c: color pulse width [ms]
τ_d: time delay between colors [ms]

INTRODUCTION

Horizontal annular flow is a dominant flow regime for heat exchanger tubing. Past work indicates that bubbles entrained in the liquid annulus may serve as secondary nucleation sites for vaporization within a film too thin for nucleate boiling to take place. For the case of a thicker condensation film, bubbles lower the resistance posed to heat transfer. Previous observations of the thin annular liquid film on an air-water loop revealed the presence of entrained bubbles. In this study, three optical methods are combined for the exploration of the bubble entrainment and transport mechanisms in air-water horizontal annular flow. The combined data should characterize the size distribution, concentration, and velocity of the bubbles.

Single pulses from a pair of xenon strobe lights provide frozen images of bubbles that are captured on digital video for concentration and size distribution determination. Two light sources are used to obtain two reflections on opposite sides of the bubble, which determine its diameter. Ensemble averaging of data from such images is performed for various flow rate settings.

Particle tracking velocimetry (PTV) provides velocity information. PTV is a well-established technique applicable to sparsely seeded flows. The low density of the seeding allows the recognition of individual particle trajectories and the varying length of the streaks provides the velocity information.

Planar laser induced fluorescence (PLIF) provides a cross-sectional view of the liquid film along planes that contain the central axis of the tube. This technique illustrates the mechanisms of bubble entrainment as well as the concentration and size distribution along the thickness of the film. Droplet impacts into the film as well as disturbance waves are better visualized using this method.

BACKGROUND

In many boiling situations, surface cavities with entrapped gas provide bubble nucleation sites. However, nucleate boiling in a thin liquid film features a secondary nucleation behavior [1,2] that effectively enhances heat transfer by creating a low thermal resistance liquid microlayer very close to the wall. Secondary homogeneous nucleation has been observed to contribute up to 40 % of the total heat flux in spray cooling experiments in which droplets impact a thin boiling liquid film [3,4].

Recent experiments [5] have challenged the importance of secondary nucleation by comparing evaporation and condensation heat transfer coefficients under identical vertical annular flow conditions. Secondary nucleation was assumed to have a small influence on condensation and a larger influence on evaporation. Secondary nucleation would then be important only if the evaporation coefficients were significantly higher than those for condensation even in the absence of wall nucleation. These experiments showed no difference between evaporation and condensation. However, these experiments did not consider that vapor bubbles could impact both evaporation and condensation similarly. Entrained bubbles may still be important if a significant concentration of them exists near the wall, lowering the effective thickness of the film for both evaporation and condensation.

Droplets, such as the ones entrained in the gas core of the annular flow, impact the liquid film surface entraining small amounts of gas that were adsorbed on their surface [6]. Another mechanism of gas entrainment in the thin film is associated with disturbance waves and their interaction with the gas core. This entrainment mechanism is not necessarily the same as for surface (oceanic) waves due to the different, more chaotic, nature of disturbance waves. Disturbance wave behavior is currently not understood well enough to be able to predict how it may act as a mechanism for gas entrainment.

EXPERIMENTAL

Air-Water Flow Loop

A 5.8 m length of clear PVC tubing (14.9 mm bore) is employed as a horizontal test section in which various stratified and annular flow regimes are established. Optical measurements are performed towards the end of the tube (about 380 L/D from the entrance) where the effects of the initial air and water injection are small. Rotameters provide the air and water volumetric flows. Temperature is monitored for both air and water just before the mixing tee at the inlet. Air pressure is monitored at the exit of the air flowmeter.

Flow Settings

The flow regimes are characterized by a modified version of the Froude number called the Froude rate F_t. The Froude rate represents a ratio of the rate of kinetic energy flowing in the gas, to the power required to "pump" liquid from the bottom to the top of the tube [7] and is defined by

$$F_t = \sqrt{\frac{W_g}{W_l}}\left(\frac{U_{sg}}{\sqrt{gd}}\right). \quad (1)$$

In general, within the annular regime, a higher Froude rate is associated with a thinner and more symmetric liquid annulus. However, the Froude rate does not specify the flow regime and it is not meant to correlate the transitions between flow regimes. The form of the flow may be different for identical values of F_t depending on the specific gas and liquid mass flow rates. The basic flow patterns covered by the current study are stratified flow, low F_t annular flow, and high F_t annular flow (all three flow patterns are achieved within the range $35 < F_t < 250$).

Single Pulsed Images

A Canon XL1 digital video camera (640x480 pixel resolution), fitted with a 95 mm macro lens, is focused on a 5 mm wide by 3.75 mm long portion of the thin liquid film (see Figure 1). A pair of xenon strobe lights is pulsed once per video frame to produce frozen images of the liquid film. The fixed, built-in pulse width of the strobe light may vary between 10 and 30 μs. Reflections are visible on opposite sides of the bubble surface, such that the bubble diameter may be measured from their separation. Bubble images from each frame are manually counted and measured with some assistance from image processing software (NIH ImageJ)[8]. Data for several frames are ensemble-averaged to obtain bubble size distribution and concentration information.

The scale for performing measurements on the images is obtained from focusing the camera on the tips of a caliper placed on the outer surface of the tube. Image processing software allows the measurement of the tip separation in pixels. This scale can be introduced into the software's measurement functions to obtain lengths or areas in physical units.

Two basic criteria are employed for differentiating air bubbles from other particulate matter. The first criterion is related to surface reflections that are visible only from the side of the bubble where light is incident. For other clear particulate matter, like glass spheres, reflections are visible both on the incident and opposite sides of the surface due to the higher index of refraction of the glass. A second criterion is provided by the fact that few or no bubbles are visible at relatively higher air flow rates.

Particle Tracking Velocimetry (PTV)

This study employs a conveniently modified source of illumination for producing streak images of the bubbles. An array of nine white, eight blue and eight red LEDs is used as the light source. The three colors are pulsed in a repetitive sequence (white, blue, red). Each color has a pulse width τ_c, with a time delay in between colors τ_d. The length of the colored streaks along a bubble trajectory provides instantaneous velocity information. The color encoding greatly assists in the interpretation of the results, since temporal and spatial ambiguities can be resolved. Same colored streaks determine a specific instant of time during the frame exposure so situations such as collisions, crossing trajectories, and parallel trajectories, which involve several bubbles, can be distinguished more precisely.

The pair of xenon strobe lights is flashed at a fraction of the LED frequency and a very short pulse width (10-30μs) to produce frozen images of the shape and size of the bubble associated to a particular trajectory. Bubble breakup, coalescence and deformation may also be detected from the frozen images.

Planar Laser Induced Fluorescence (PLIF)

A laser light sheet les than 1 mm thick (λ=532 nm, Nd:YAG) is used to obtain cross sections of the liquid film (see Figure 2). A fluorescent dye (Rhodamine B) is mixed with the water. A single pulse from the laser excites the dye molecules, which subsequently fluoresce with an emission peak at λ=565 nm. With adequate optical filtering (long pass or narrow band filters), only the light emitted from the liquid phase reaches the camera. The freezing of instantaneous images is accomplished through shuttering of the camera. A scientific grade CCD camera with a mechanical shutter is used for this purpose. For the slower flows, the short duration of the detectable fluorescence is enough to freeze the image without fast shuttering.

RESULTS AND DISCUSSION

Single Pulsed Images

Bubbles are easily visualized on each video frame as pairs of top and bottom reflections. The separation between pairs is a good indication of the diameter of the bubbles. Figure 3 is a sample image, cropped from a single video frame. F_t is 53.69 for air and water flow rates of 200 l/min and 200 cm^3/min respectively. The horizontal scale of the cropped image is 10 mm with a resolution of 58.43 pixels/mm. The contours of the four bubbles appearing in the image were traced for clarity. The corresponding diameters are 0.33, 0.57, 0.62 and 0.77 mm (from left to right). At this same resolution, bubbles an order of magnitude smaller can still be detected but not accurately measured due to the uncertainty associated with manually locating the reflection edges.

At higher values of F_t, the waviness of the film surface is about an order of magnitude lower than the frame dimensions, so that detecting individual bubbles becomes increasingly challenging.

Statistical data for the size distribution and concentration of bubbles was gathered for six different F_t values. A minimum of 30 video frames was ensemble averaged for each data point. Figure 4 shows the mean values of the bubble diameter and concentration. The latter is expressed as number of bubbles per frame. The data points have associated scatter bars corresponding to +/- one standard deviation of the distribution.

Bubble sizes are on the order of magnitude of the thickness of the liquid film. An interesting behavior is observed regarding the scatter. Large scatters on the size distribution are paired with smaller scatters for concentration and vice versa. Also, the existence of a significant amount of scatter in the concentration data indicates that bubble entrainment is a periodic process. This behavior can be explained if disturbance waves are the principal source of bubble entrainment. Few or no bubbles are visible right before a disturbance wave, while a high concentration exists during and right after it passes. There is an inverse relation between mean concentration and mean size of bubbles as shown in Figure 5.

Figure 6 is a represents a multimodal distribution for bubble size. The lower modes, which correspond to a larger bubble sizes, may be composed of recently entrained bubbles while the highest mode may be determined by the stable size of bubbles after breakup.

Particle Tracking Velocimetry (PTV)

In addition to top and bottom reflections, which appear several times along the trajectory of the bubble, the trajectory itself is traced by the three-colored pattern of streaks. Again, for higher F_t values, measurements are made more difficult because of the intricate film structures. Lower contrast of the streaks against the background impedes the simultaneous use of the xenon strobe lights for the higher F_t settings.

Figure 7 was cropped from a single video frame at F_t = 53.69 for air and water flow rates of 200 l/min and 200 cm^3/min respectively. The image portrays two bubbles describing nearly parallel trajectories. The bubbles have diameters of 0.78 mm and 0.43 mm and their approximate contours have been traced. The first flash of the strobe light (position 1) shows the big bubble lagging behind the smaller one as they move from left to right. By the time they reach position 3, the big bubble has caught up with the smaller bubble. This situation exemplifies the observed tendency of larger bubbles to travel faster than smaller bubbles within the liquid film. Thus, larger bubbles may travel farther away from the tube wall where higher velocities are expected. Direct measurements of the color streaks together with the value of τ_c (0.4 ms) provide an average speed of 0.58 m/s for the larger bubble on Figure 4 and 0.46 m/s for the smaller one.

The value of the three-color encoding of the streaks is evidenced by cases such as the one depicted in Figure 8. Three bubbles describe simultaneous helical trajectories. However, the previous assertion could not be made without the color encoding. Straight lines that intersect streaks corresponding to a specific instant of time have been added for clarity. The bubbles do not collide although the three 2D traces seem to intersect at one point for the same instant of time. That is precisely the instant when the line that joins the three centers is aligned with the direction of view during the helical 3D trajectory they describe.

Other events such as the burst of a slowly moving bubble when it reaches the surface of the film may also be documented (Figure 9). The resulting concentric ripples have their common center at the endpoint of the bubble trajectory.

Planar Laser Induced Fluorescence (PLIF)

The PLIF technique is limited in the case of round tubes by the critical angle for reflection at the inner tube wall. Due to this limitation, PLIF images are dark up to about 1mm away form the tube wall. Using Fluorinated Ethylene Propylene (FEP), which has an index of refraction closer to that of water, instead of PVC may improve the situation reducing the dark band to about 0.06 mm. The dark band is thicker than most liquid films for the annular regime of air-water flow.

Figure 10 shows a PLIF image of the thicker film produced by a stratified flow regime. The bubbles cut by the light sheet appear as dark spots. A shadow region above the dark spots is also visible. PLIF images require careful interpretation since dark spots may not correspond to the full diameter of the bubble and some bubbles may be hidden in the shadow region produced by other bubbles.

CONCLUSIONS

- The results obtained up to the moment demonstrate the capability of two of three experimental methods to provide estimates of bubble size, concentration and velocity. They are successful for the low Froude rate settings. However, they require a higher resolution and a brighter, more concentrated illumination from the LED array to produce comparable results at higher Froude rates, where scattering, smaller bubble size and reduced scale flow structures are a problem. There is a significant imprecision associated with the manual location of reflection edges during the measurements. Resolution should be increased for smaller, slower moving bubbles.
- Scatter in concentration results indicates disturbance waves may be the predominant entrainment mechanism. Multimodal size distributions may correspond to initial entrainment size and final stable size of bubbles after breakup. The total entrained volume of gas appears to be inversely proportional to F_t.
- Bubble speeds in the order of 0.5 m/s were measured and larger bubbles appear to travel at higher speeds than smaller bubbles
- Some features of the flow such as helical trajectories and bubble bursts are commonly observed on PTV measurements.
- Future work will include studying the bubble behavior at various circumferential locations and automating the processing of images for bubble size, concentration and velocity measurements.

ACKNOWLEDGEMENTS

The authors appreciate the financial support for this project provided by the University of Wisconsin and the National Science Foundation under award number CTS-0134510.

REFERENCES

[1] Mesler, R.B., "Improving nucleate boiling", *Pool and External Flow Boiling*, V.K. Dhir & A.E. Bergles, Editors, ASME Press, pp. 43-47,1992.
[2] Mesler, R.B., "A mechanism supported by extensive experimental evidence to explain high heat fluxes observed during nucleate boiling", *AIChE Journal* 22, No. 2, pp. 246-252, 1976
[3] Rini, D.P., Chen, R.R., Chow, L.C., "Bubble behavior and nucleate boiling heat transfer in saturated FC-72 spray cooling", *J. Heat Transfer* 124, pp. 63-72, 2002
[4] Yang, J., Chow, L.C., Pais, M.R.,"Nucleate Boiling Heat Transfer in Spray Cooling", *Journal of Heat Transfer* 118, pp. 668-671, 1996
[5] Sun, G., Hewitt G.F., "Evaporation and condensation of steam water in a vertical tube", *Nuclear Engineering and Design* 207, pp. 137-145, 2001.
[6] Elmore, P.A., Chahine, G.L., Oguz, H.N., "Cavity and flow measurements of reproducible bubble entrainment following drop impacts", *Experiments in Fluids* 31, pp. 664-673, 2001.
[7] Shedd, T.A.,"Characteristics of the liquid film in horizontal two-phase annular flow", Ph.D. Thesis, University of Illinois at Urbana-Champaign, pp. 25, 2001.
[8] Rasband, W., *Image J 1.26t*, National Institutes of Health ,USA,http://rsb.info.nih.gov/ij/

FIGURES

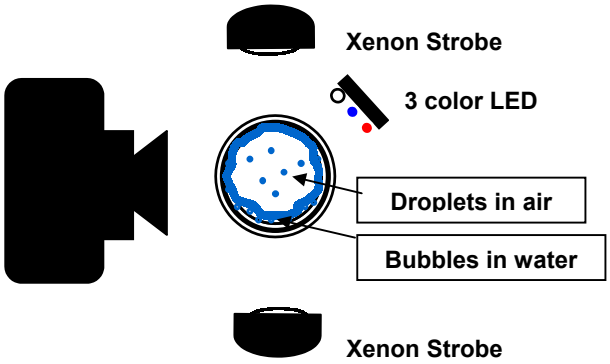

Figure 1: Scheme of lighting and camera setup for single pulsed images and PTV.

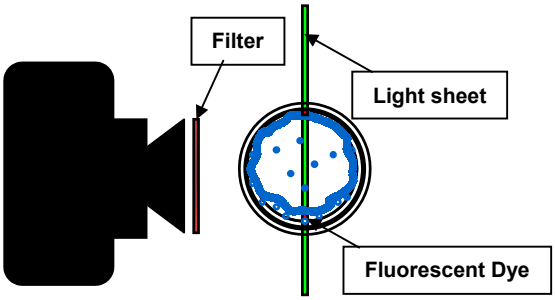

Figure 2: Scheme of lighting and camera setup for PLIF.

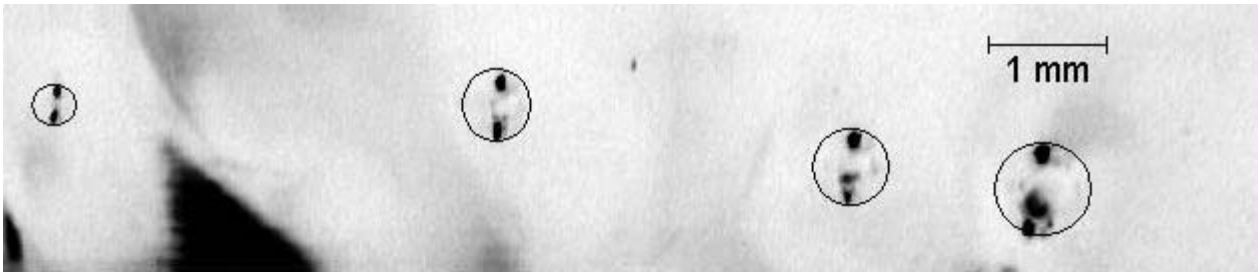

Figure 3: Sample of single pulsed image.

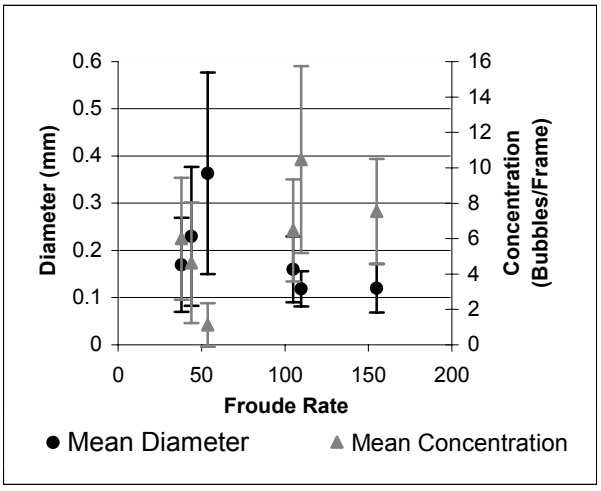

Figure 4: Mean diameter and mean concentration for various values of F_t

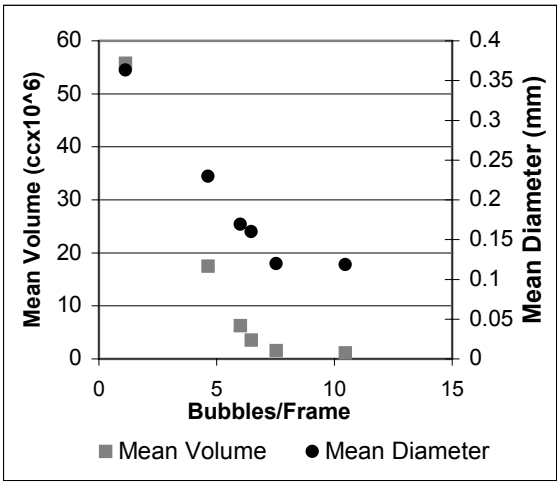

Figure 5: Mean volume and mean diameter vs. concentration

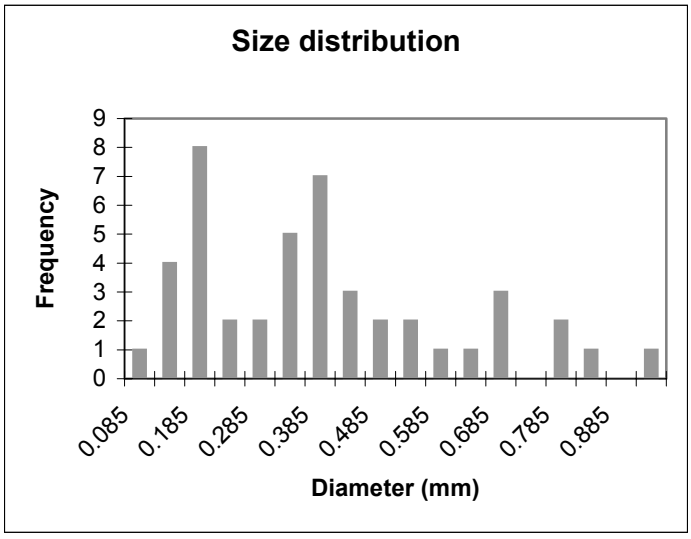

Figure 6: Multimodal size distribution for F_t =53.7

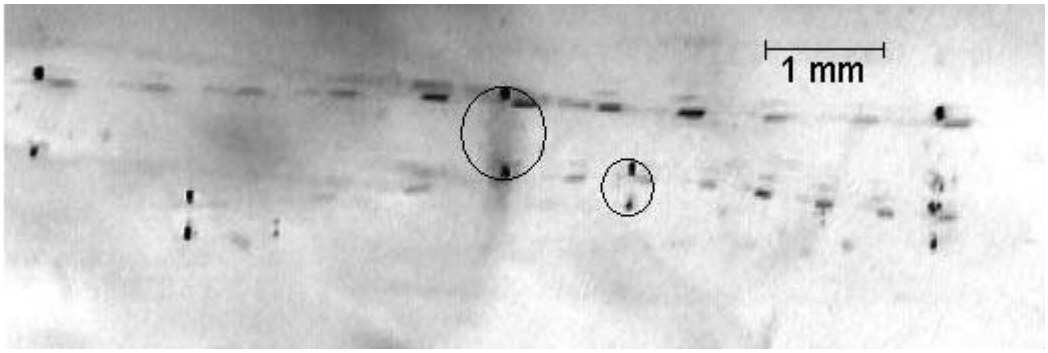

Figure 7: Sample PTV image

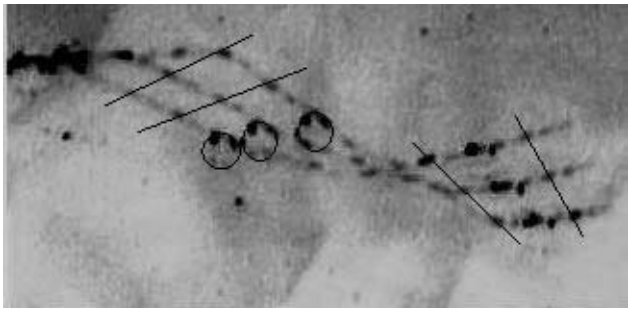

Figure 8: PTV image of three bubbles describing simultaneous helical trajectories

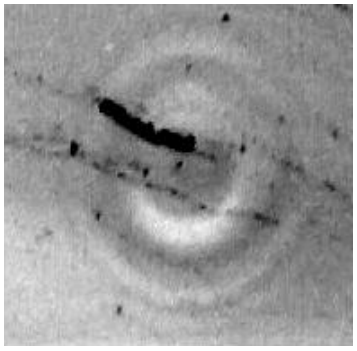

Figure 9: PTV image of a bubble bursting at the film surface

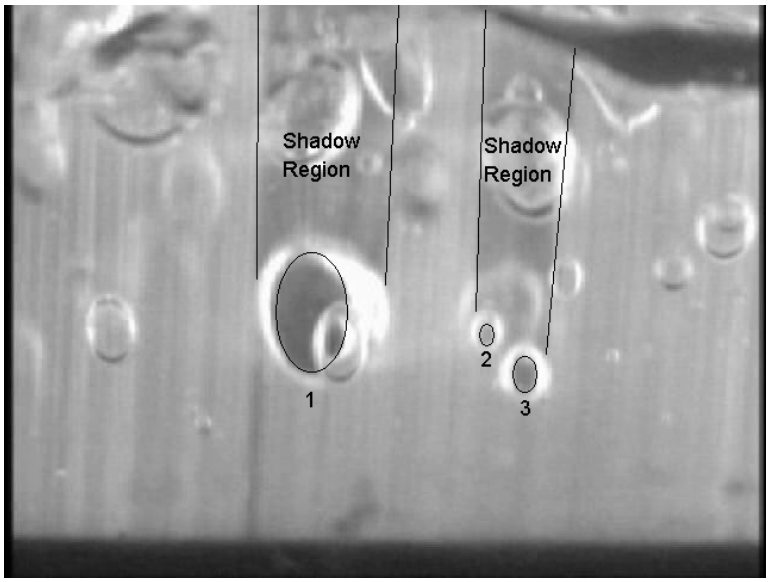

Figure 10: PLIF image of stratified flow. Three dark spots and the corresponding shadow regions have been traced for clarity